Width dependence of quantum lifetimes in $GaAs/Al_xGa_{1-x}As$ heterostructures

K.-H. Yoo
Korea Research Institute of Standards and Science, Yusung, P.O. Box 102, Taejon 305-600, Korea

J. W. Park and J. B. Choi
Department of Physics, Chungbuk National University, Cheongju 360-763, Korea

H. K. Lee and J. J. Lee
Electronics and Telecommunications Research Institute, Yusung, P.O. Box 106, Taejon 305-600, Korea

T. W. Kim
Department of Physics, Kwangwoon University, Seoul 139-701, Korea
(Received 17 November 1995)

We have studied the channel width dependence of quantum lifetimes τ_q (or equivalently the quantum mobilities $\mu_q = e\tau_q/m^*$) for samples with the widths w of 2–50 μm fabricated from three $GaAs/Al_xGa_{1-x}As$ wafers. μ_q estimated from the amplitude of Shubnikov–de Haas oscillations is found not to be affected by the asymmetry of Shubnikov–de Haas peaks and the boundary scattering observed in narrow samples. However, the two- to one-dimensional crossover occurring at $w < L_T$ (thermal diffusion length) leads to the reduction of μ_q. In addition, we have also carried out similar measurements with the sample illuminated with a red light-emitting diode. The results obtained from the illuminated samples confirm those from the unilluminated samples. [S0163-1829(96)00624-8]

I. INTRODUCTION

In the transport theory one must deal with two different characteristic times—a quantum lifetime (single-particle relaxation time) τ_q and a transport lifetime τ_{tr}. τ_{tr} is related to the two-electron correlation function that defines the conductivity and is given by

$$\sigma = N_s e \mu_{tr} = N_s e^2 \tau_{tr}/m^*, \tag{1}$$

where N_s is the two-dimensional (2D) sheet carrier density, μ_{tr} is the transport mobility, and m^* is the electron effective mass, whereas τ_q, which is determined by the one-electron Green's function of the coupled electron-impurity system,[1] is related to the half-width Γ of the broadened Landau level through $\Gamma = \hbar/2\tau_q$. For a short-range scattering potential such as a Si metal-oxide-semiconductor field-effect transistor (MOSFET) τ_q and τ_{tr} are approximately equal,[2] but for $GaAs/Al_{1-x}Ga_xAs$ heterostructures, where the dominant scattering mechanism is the long-range scattering associated with the ionized donors which are spatially separated from the 2D electron gas and which produce predominantly small-angle scattering,[3,5] τ_{tr} can be considerably greater than τ_q.[3–5]

Several studies of τ_q have been reported in $GaAs/Al_xGa_{1-x}As$ heterojunctions with different N_s and μ_{tr},[3–5] and in narrow wires.[6,7] However, the channel width dependence of τ_q has never been systematically investigated. In high-mobility narrow samples, where the mean free path often exceeds the sample width w, the magnetoresistivity is affected by the boundary scattering[8] and the asymmetry of the Shubnikov–de Haas (SdH) spin-split peaks is observed.[9,10] Furthermore, if the sample width becomes less than the thermal diffusion length L_T defined by $L_T = \pi(\hbar D/kT)^{1/2}$, where $D = 1/2 v_F^2 \tau$ is the diffusion constant and v_F is the Fermi velocity, the electron-electron interactions cross over from 2D to 1D.[8] These features observed in narrow samples may influence Γ and τ_q, so we have investigated the channel width dependence of τ_q by measuring τ_q of samples with $w = 2-50$ μm and presented the results in this paper.

II. EXPERIMENTS

In order to study the channel width dependence of quantum lifetime τ_q, six-bridged Hall bars with different channel widths $w = 2-50$ μm but the same voltage-probe space $L = 100$ μm were fabricated by standard photolithographic technique from three different $GaAs/Al_xGa_{1-x}As$ ($x = 0.3$) wafers grown by molecular-beam epitaxy, the details of which are given in Table I. The chemical etching was carried out by immersing samples in a reagent of H_3PO_4:H_2O_2:H_2O=1:1:20 for 30 s. Since L_T is larger than 2 μm for all wafers, we expect to observe a dimensional crossover at $T < 4.2$ K. The transport mobility μ_{tr} was determined from the zero-field resistivity ρ_0 with N_s obtained from the periodicity of the low-field SdH oscillations. N_s and μ_{tr} are almost the same for $w \geq 4$ μm, but for $w = 2$ μm they are slightly decreased. The magnetoresistivity measurements were carried out in a ^{4}He cryostat equipped with a supercon-

TABLE I. Sample parameters and the thermal diffusion length.

	N_s (10^{15} m^{-2})	μ_{tr} (m^2/V s)	Space (Å)	L_T (μm)
Wafer I	3.3	100	200	9.3
Wafer II	3.1	62	300	7.1
Wafer III	2.9	30	170	4.8

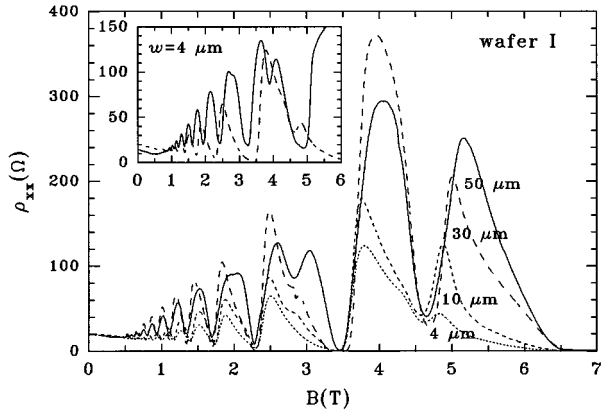

FIG. 1. The magnetoresistivity ρ_{xx} at $T=1.5$ K as a function of the magnetic field B for the samples having various widths (wafer I). The inset is the plot of ρ_{xx} vs B for the sample with $w=4$ μm (wafer I), where the dashed curve represents the data of the sample cooled in the dark and the solid one the data of the sample illuminated with a red LED.

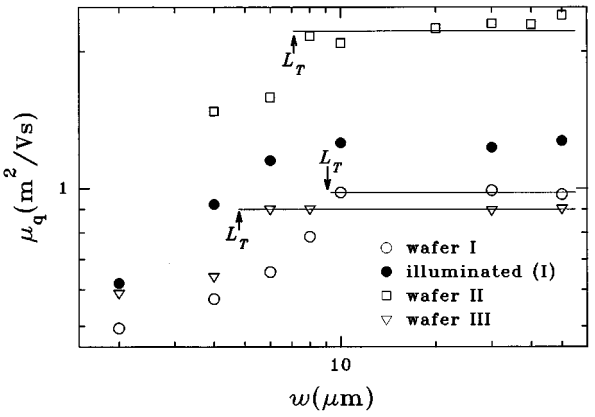

FIG. 2. The quantum mobility μ_q at $T=1.5$ K as a function of channel width w for the samples from wafer I (○), wafer II (□), and wafer III (▽), and for the samples (wafer I) illuminated with a red LED (●). The arrows indicate the thermal diffusion length L_T given by $L_T=\pi(\hbar D/kT)^{1/2}$, where D is the diffusion constant and v_F is the Fermi velocity.

ducting magnet and the standard low-frequency lock-in technique was used with $10<I<50$ nA at 33 Hz. The sweeping rate of the magnetic field was such that there were typically 1000 data points within 1 T.

Quantum lifetimes τ_q have been determined from Dingle plots.[11] The amplitude $\Delta\rho$ of the SdH oscillations is given by[4]

$$\Delta\rho=4\rho_0\frac{\chi}{\sinh\chi}\exp\left[-\frac{\pi}{\omega_c\tau_q}\right], \tag{2}$$

where ρ_0 is the zero-field resistivity, ω_c the cyclotron frequency, and $\chi=2\pi^2kT/\hbar\omega_c$. If the logarithm of $\Delta\rho$ divided by $4\rho_0\chi/\sinh\chi$ is plotted against $1/B$, the slope gives $1/\tau_q$ directly with an intercept of 1. However, the actual measurements give the magnetoresistivity consisting of the purely oscillatory component of the magnetoresistivity $\Delta\rho$ and the background which is quadratic in B and which is believed to be associated with electron-electron interactions.[12] Therefore we extracted the purely oscillatory component $\Delta\rho$ from the data by using the Fourier-filtering technique and estimated τ_q using Eq. (2).

III. RESULTS AND DISCUSSION

Figure 1 shows the magnetoresistivity ρ_{xx} at $T=1.5$ K as a function of the magnetic field B for the samples having several widths (wafer I). For $w\leqslant 30$ μm, the asymmetric SdH peaks are observed as reported by others,[9,10] whereas the typical SdH oscillations are found for $w=50$ μm. Although the asymmetric SdH oscillation has been suggested to be due to the edge-state transport,[13] since τ_q is closely related to the half-width of the broadened Landau level, we have calculated τ_q for $w=30$ and 50 μm and presented the results in Fig. 2, where the quantum mobility μ_q is obtained from τ_q via the relation $\mu_q=e\tau_q/m^*$ ($m^*=0.069m_0$). Almost identical values of μ_q are found for both samples, indicating that μ_q may not be related to the origin leading to the asymmetric line shapes of SdH oscillation. In the samples from wafer II we have found the asymmetric SdH oscillations for $w\leqslant 10$ μm and obtained almost the same values of μ_q for $w\geqslant 10$ μm as shown in Fig. 2. This confirms that μ_q is not affected by the asymmetry of SdH oscillations. On the other hand, the samples from wafer III, which has relatively low mobility, exhibited no sawtoothed SdH peaks even for $w=2$ μm.

Figure 3 shows the magnetoresistivity ρ_{xx} at $T=1.5$ K against B^2 for the samples with $2\leqslant w\leqslant 30$ μm (wafer I). For $w=30$ μm ρ_{xx} is linear to B^2 in the range of $0<B^2<0.1$ T^2. This parabolic ρ_{xx} has been explained by the conductivity correction due to the electron interaction effect.[12] For $w\leqslant 10$ μm, on the other hand, ρ_{xx} changes its slope around B_c, whose value increases as w decreases. Choi, Tsui, and Palmateer[8] have observed similar behaviors and suggested that the drop of ρ_{xx} below B_c is attributed to the boundary scattering and the B^2 dependence of ρ_{xx} above B_c to the electron-electron interaction. It implies that the boundary scattering plays an important role in narrow samples ($w\leqslant 10$ μm), while it is negligible in wide samples. In order to investigate whether the boundary scattering affects μ_q or not, we have estimated μ_q of the samples with $w=10$ and 30 μm. As presented in Fig. 2, two samples have approximately

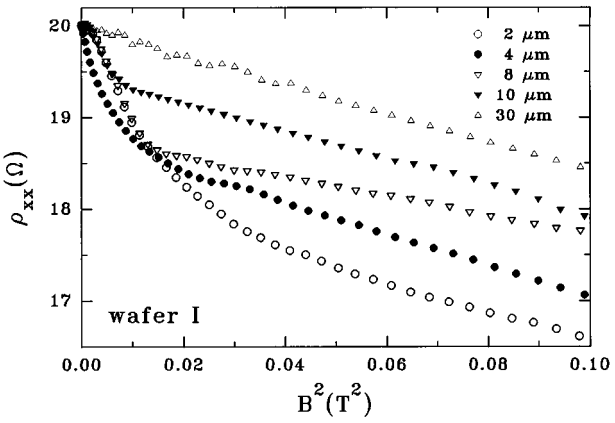

FIG. 3. Plot of ρ_{xx} vs B^2 at $T=1.5$ K for the samples with various widths (wafer I).

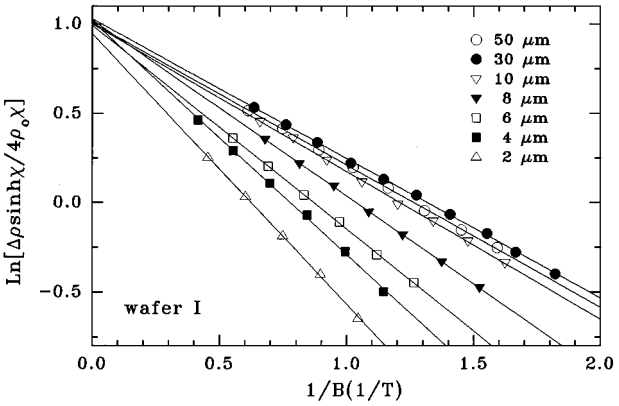

FIG. 4. Plot of $\ln[\Delta\rho \sinh \chi/4\rho_0\chi]$ vs $1/B$ at $T=1.5$ K for the samples with various widths (wafer I).

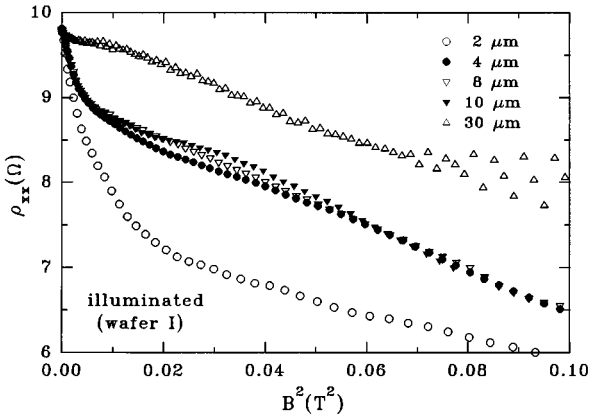

FIG. 5. Plot of ρ_{xx} vs B^2 at $T=1.5$ K for the illuminated samples with various widths (wafer I).

identical values of μ_q, suggesting that μ_q is not influenced by the boundary scattering. If the boundary scattering is effective when w is smaller than or comparable to the cyclotron radius given by $l_c=\hbar k_F/eB$, where k_F is the Fermi wave vector, the effects of boundary scattering may diminish in the magnetic field range where the SdH oscillations appear. Then, no influence of boundary scattering on μ_q may be understood. Indeed, B_c in Fig. 3 is roughly proportional to $1/w$, although B_c is larger than $\hbar k_B/ew$.

Above B_c, the slope of ρ_{xx} vs B^2 is nearly constant for $w \geqslant 8$ μm, whereas for $w \leqslant 6$ μm the slope becomes steep with decreasing w. Since L_T of wafer I is about 9.3 μm and it is known that the slope of ρ_{xx} vs B^2 is inversely proportional to the width in 1D, while the slope of ρ_{xx} vs B^2 is independent of w in 2D,[8] the change in the slope of ρ_{xx} vs B^2 below 8 μm is considered to result from the dimensional crossover from 2D to 1D. Wafers I and II have also exhibited similar changes in the slope of ρ_{xx} vs B^2 above B_c for $w \leqslant 6$ and 4 μm, respectively. Similarly to wafer I, the values of $w=6$ and 4 μm are comparable to L_T of each sample.

Figure 4 shows the Dingle plots of $\ln[\Delta\rho_{xx} \sinh \chi/4\rho_0\chi]$ vs $1/B$ at $T=1.5$ K for the samples with various widths (wafer I). The straight lines are obtained and their intercepts converge to a value which is slightly larger than 1. This indicates that they are ''good'' Dingle plots.[5] In Fig. 2 the channel width dependences of μ_q at 1.5 K are shown for the samples fabricated from wafers I–III. The filled symbols in Fig. 2 represent the results of the samples (wafer I) illuminated with a red light-emitting diode (LED), which will be discussed later. For all samples μ_q decreases with reducing w below L_T, while μ_q is approximately independent of w above L_T. The comparison with the results in Fig. 3 suggests that the reduction of μ_q for $w<L_T$ may be ascribed to the dimensional crossover from 2D to 1D. As far as we know, μ_q has not been calculated in 1D, where the screened Coulomb potential describing the interaction between an electron and an impurity may need to be modified, so that the reduction of μ_q for $w<L_T$ cannot be explained quantitatively. However, since μ_q is sensitive to all scattering events, unlike $\mu_{\rm tr}$ which is independent of the scattering angle, and the scatterings are more restricted in 1D and 2D, it is speculated that $\mu_{\rm tr}/\mu_q$ may be larger in 1D than 2D.

Besides the above measurements performed with the samples cooled in the dark, we have also carried out the measurements using the samples (wafer I) illuminated with a red LED. The illumination increased N_s and $\mu_{\rm tr}$ to $N_s=4.4\times10^{15}$ m^{-2} and $\mu_{\rm tr}=183$ m^2/V s, respectively. In the inset of Fig. 1, the plot of ρ_{xx} vs B is displayed for the illuminated sample with $w=4$ μm. On the contrary to the unilluminated sample, the sawtoothed SdH oscillations are not observed even for $w=4$ μm. When the samples were illuminated with a red LED, only the sample with $w=2$ μm exhibited the asymmetry of SdH peaks.

Figure 5 shows the plots of ρ_{xx} vs B^2 for the illuminated samples (wafer I). Similarly to the unilluminated samples, the drops of ρ_{xx}, which are caused by the boundary scattering, are found for $w \leqslant 10$ μm. However, the slope of ρ_{xx} vs B^2 above B_c shows different behaviors from the unilluminated samples. On the contrary to the unilluminated samples which show the transition in the slope of ρ_{xx} vs B^2 at around $w=10$ μm in Fig. 3, the slope of ρ_{xx} vs B^2 in the illuminated samples is nearly constant for $w \geqslant 4$ μm. This implies that the effective width may be increased by illumination so that the dimensional crossover occurs at the narrower width. For $w \geqslant 6$ μm μ_q of the illuminated samples represented by the filled symbols in Fig. 2 is nearly independent of w, while for $w \leqslant 4$ μm μ_q decreases with decreasing w. This confirms that the boundary scattering does not influence μ_q and the reduction of μ_q is associated with the 2D-to-1D transition although the illuminated sample with $w=4$ μm, whose slope of ρ_{xx} vs B^2 above B_c is almost the same as that of $w \geqslant 6$ μm, shows a smaller value of μ_q than the illuminated samples with $w \geqslant 6$ μm.

IV. CONCLUSION

The width dependences of μ_q (or equivalently τ_q) were investigated for the samples with $w=2-50$ μm fabricated from three wafers. We have observed the asymmetric SdH peaks in narrow samples ($w \leqslant 30$ μm for wafer I and $w \leqslant 10$ μm for wafer II) and the drop of ρ_{xx} near the zero field due to the boundary scattering for $w \leqslant 10$ μm. However, μ_q is found to be almost constant for the samples having channel width larger than L_T (9.3 μm for wafer I, 7.1 μm for wafer II, and 4.8 μm for wafer III), implying that neither asymmetric SdH oscillations nor the boundary scattering affect μ_q. Below L_T, however, μ_q decreases with reducing w. Since

the dimensional transition from 2D to 1D is expected to occur at $w \approx L_T$ and the slope of ρ_{xx} vs B^2 above B_c shows the 1D characteristics for $w < L_T$,[8] the reduction of μ_q is considered to be due to the dimensional crossover from 2D to 1D. In addition to the above measurements, we have also carried out the measurements with the samples (wafer I) illuminated with a red LED. In the illuminated samples the dimensional crossover is observed to occur at the narrower width compared with the unilluminated samples, probably because of the increased effective width by illumination. However, μ_q estimated from the illuminated samples exhibits similar behaviors to that of the unilluminated samples.

ACKNOWLEDGMENT

This work is supported by the Ministry of Science and Technology of the Republic of Korea.

[1] S. Das Sarma and B. Vinter, Phys. Rev. B **24**, 549 (1981); Surf. Sci. **113**, 176 (1982).
[2] F. F. Fang, A. B. Fowler, and A. Hartstein, Phys. Rev. B **16**, 4446 (1977).
[3] J. P. Harrang, R. J. Higgins, R. K. Goodall, P. R. Jay, M. Laviron, and P. Delescluse, Phys. Rev. B **32**, 8126 (1986).
[4] P. T. Coleridge, R. Stoner, and R. Fletcher, Phys. Rev. B **39**, 1120 (1989).
[5] P. T. Coleridge, Phys. Rev. B **44**, 3793 (1991).
[6] A. D. C. Grassie, K. M. Hutchings, M. Lakrimi, C. T. Foxon, and J. J. Harris, Phys. Rev. B **36**, 4551 (1987).
[7] K. Ishibashi, Y. Aoyagi, S. Namba, Y. Ochiaj, M. Kawabe, and K. Gamo, Superlatt. Microstruct. **11**, 195 (1992).
[8] K. K. Choi, D. C. Tsui, and S. C. Palmateer, Phys. Rev. B **33**, 8216 (1986).
[9] H. Z. Zheng, K. K. Choi, D. C. Tsui, and G. Weimann, Phys. Rev. Lett. **55**, 1144 (1985).
[10] R. J. Haug, K. v. Klitzing, and K. Ploog, Phys. Rev. B **35**, 5933 (1987).
[11] T. Ando, J. Phys. Soc. Jpn. **37**, 1233 (1974).
[12] M. A. Paalanen, D. C. Tsui, and J. C. M. Hwang, Phys. Rev. Lett. **51**, 2226 (1983).
[13] R. J. Haug, Semicond. Sci. Technol. **8**, 131 (1993).